TU/e EINDHOVEN UNIVERSITY OF TECHNOLOGY

Convergence properties of the local defect correction method for parabolic problems

Citation for published version (APA):
Minero, R., Morsche, ter, H. G., & Anthonissen, M. J. H. (2005). *Convergence properties of the local defect correction method for parabolic problems*. (CASA-report; Vol. 0540). Technische Universiteit Eindhoven.

Document status and date:
Published: 01/01/2005

Document Version:
Publisher's PDF, also known as Version of Record (includes final page, issue and volume numbers)

Please check the document version of this publication:

• A submitted manuscript is the version of the article upon submission and before peer-review. There can be important differences between the submitted version and the official published version of record. People interested in the research are advised to contact the author for the final version of the publication, or visit the DOI to the publisher's website.
• The final author version and the galley proof are versions of the publication after peer review.
• The final published version features the final layout of the paper including the volume, issue and page numbers.

Link to publication

General rights
Copyright and moral rights for the publications made accessible in the public portal are retained by the authors and/or other copyright owners and it is a condition of accessing publications that users recognise and abide by the legal requirements associated with these rights.

• Users may download and print one copy of any publication from the public portal for the purpose of private study or research.
• You may not further distribute the material or use it for any profit-making activity or commercial gain
• You may freely distribute the URL identifying the publication in the public portal.

If the publication is distributed under the terms of Article 25fa of the Dutch Copyright Act, indicated by the "Taverne" license above, please follow below link for the End User Agreement:

www.tue.nl/taverne

Take down policy
If you believe that this document breaches copyright please contact us at:

openaccess@tue.nl

providing details and we will investigate your claim.

Download date: 16. Nov. 2023

Convergence properties of the local defect correction method for parabolic problems

R. Minero*, H.G. ter Morsche, M.J.H. Anthonissen

Eindhoven University of Technology
Department of Mathematics and Computer Science
P.O. Box 513, 5600 MB Eindhoven, The Netherlands
e-mail r.minero@tue.nl

This paper is devoted to the study of the convergence properties of the Local Defect Correction (LDC) technique for parabolic problems presented in [14]. We derive a general expression for the iteration matrix of the method and, for a one-dimensional heat equation, we study its properties analytically. Numerical experiment are in agreement with the theoretical results.

1 Introduction

Solutions of Partial Differential Equations (PDEs) are often characterized, at each time, by regions where spatial gradients are large compared to those in the rest of the domain, where the solution presents a relatively smooth behavior. Examples are frequently encountered in the area of shock hydrodynamics, transport of passive tracers in turbulent flow fields, combustion processes, etc. An efficient numerical solution of this kind of problems requires the usage of adaptive grid techniques. In adaptive grid methods, a fine grid spacing and a relatively small time step are adopted only where the relatively large variations occur, so that the computational effort and the memory requirements are minimized.

An adaptive grid technique of particular interest is the Local Defect Correction (LDC) method. LDC was first introduced in [12] for solving elliptic partial differential equations. LDC has then been studied in combination with different discretization techniques: finite differences in [9, 10], finite volumes in [1, 5] and finite elements in [23]. In [11, 16] the method is applied with different grid types, while in [2] it is extended to include multiple levels of refinement, domain decomposition and regridding.

In [14] LDC is generalized to solve parabolic partial differential equations. In a time-dependent setting the method works as follows: first a time step is performed on a global coarse grid. The global solution at the new time level provides artificial boundary conditions on a local fine grid, which is adaptively placed where the high activity occurs. A solution is then computed locally, possibly with a smaller time step

*R. Minero was sponsored by the Netherlands Organisation for Scientific Research (NWO) under Computational Science research grant 635.000.002.

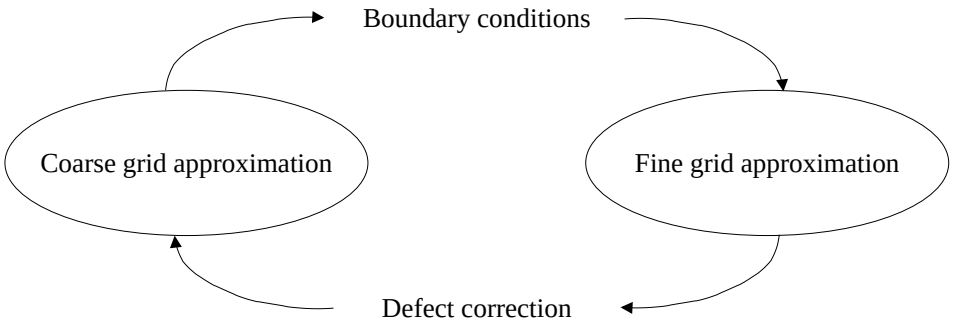

Figure 1: Scheme of the LDC iteration at a generic time step.

than the one adopted on the global grid. At this point the local approximation provides an estimate of the coarse grid discretization error or defect. The defect, added to the right hand side of the coarse grid problem, leads to determining a more accurate (both in space and time) global approximation of the solution. This can now be used to update the boundary conditions locally and the entire procedure can be repeated again until convergence. At each time step LDC is thus an iterative process in which a global and a local approximation of the solution progressively improve each other. The scheme of the LDC iteration is represented in Figure 1. In [15] the defect term is adapted to a finite volume discretization in order to have discrete conservation on the composite grid.

One of the main advantages of the method is that the global and the local grid can always be uniform structured grids. With this respect LDC is similar to the Local Uniform Grid Refinement (LUGR) method presented and analyzed in [20–22]. An LUGR based strategy for electrochemical applications is proposed in [6]. LDC, though, differs from LUGR because in LUGR the local solution does not improve the solution globally through the defect correction. For this reason, as illustrated in [14], LDC turns out to be a more robust method than LUGR. However, apart from making LDC more robust, the extra corrections involve more computational work. For LDC to be competitive with other techniques, it is thus desirable that only a small number of iterations are necessary at every time step. This paper is therefore focused on the convergence properties of the LDC method for time-dependent problems. In particular, we are interested in investigating the dependency of the LDC convergence rate on the time step for the coarse grid problem.

The convergence properties of LDC have been previously studied for stationary problems. With reference to a two-dimensional Poisson equation, in [3] it is proved that iteration errors reduce proportionally to H^2, where H is the coarse grid size. In [18] a convergence analysis is carried out for a case where the local domain has an annular shape. In general, even for rather complicated applications, it is observed by many authors (see again [1, 2, 9, 11, 16]) that one or two iterations are usually sufficient for convergence.

This paper is structured as follows: in Section 2 the LDC method for parabolic partial differential equations is presented. In Section 3 we give an expression for the LDC iteration matrix. In Section 4 we introduce a one-dimensional model problem and, for this model problem, in Section 5 we analyze the iteration matrix properties and asymptotics. At the end, the theoretical results are verified by means of numerical experiments (Section 6), while Section 7 is devoted to conclusions.

2 The LDC method for parabolic problems

In this section we present the LDC method for solving parabolic problems. Our focus is to describe the LDC iteration that takes place at a generic time step. At this generic time step, we assume the local fine grid to be given and placed in the region of the global domain where the big variations in the solution occur. For this reason the notation used in this paper is simplified with respect to [14], where also regridding (i.e. fine grid adaptation to follow the high activity movements) is taken into account.

We consider the following two-dimensional problem

$$\begin{cases} \dfrac{\partial u(\mathbf{x},t)}{\partial t} = Lu(\mathbf{x},t) + f(\mathbf{x},t), & \text{in } \Omega \times \Theta, \\ u(\mathbf{x},t) = \psi(\mathbf{x},t), & \text{on } \partial\Omega \times \Theta, \\ u(\mathbf{x},0) = \varphi_0(\mathbf{x}), & \text{in } \Omega \cup \partial\Omega, \end{cases} \tag{2.1}$$

where Ω is a spatial domain, $\partial\Omega$ its boundary and Θ the time interval $(0, t_{end}]$. Moreover, L is a linear elliptic operator, f a source term, ψ a Dirichlet boundary condition and φ_0 a given initial condition.

Problem (2.1) has to be discretized in space and time in order to be solved numerically. For that we introduce the global uniform coarse grid (grid size H) Ω^H and the time step Δt. We assume that u has, at each time level, a region of high activity that covers a small part of Ω. Therefore, at time $t_n := n\Delta t$, a coarse grid approximation computed with a time step Δt might be not adequate enough to represent $u(\mathbf{x}, t_n)$. In order to better capture the local high activity, we also solve the problem on local uniform fine grid (grid size $h < H$), which we denote by Ω_l^h. On Ω_l^h the time integration is performed using a time step $\delta t = \Delta t/\tau$, with τ an integer ≥ 1. As already mentioned before, the local solution will be used to improve the global approximation through a defect correction.

In the remainder of this section we will assume that a solution $u^{H,h,n-1}$ is known at a generic time t_{n-1} on the composite grid $\Omega^{H,h} := \Omega^H \cup \Omega_l^h$, see Figure 2. For $n > 1$, its expression is given by

$$u^{H,h,n-1} := \begin{cases} u_l^{h,n-1}, & \text{in } \Omega_l^h, \\ u^{H,n-1}, & \text{in } \Omega^H \setminus \Omega_l^h, \end{cases} \tag{2.2}$$

where $u_l^{h,n-1}$ and $u^{H,n-1}$ are a local and a global approximation of $u(\mathbf{x}, t_{n-1})$ respectively. If $n = 1$, $u^{H,h,n-1}$ is expressed through the initial condition φ_0. Our goal is to compute an approximation of the solution at the new time level t_n on the composite grid $\Omega^{H,h}$ by means of LDC.

A coarse grid approximation at t_n, we call it $u_0^{H,n}$, can be computed applying the backward Euler method to the PDE in (2.1). While other implicit time integration schemes could also be adopted, the usage of explicit time integrators on the global grid is not of interest in LDC; this is discussed in [14]. We obtain

$$(I - \Delta t\, L^H)\, u_0^{H,n} = u^{H,h,n-1}|_{\Omega^H} + f^{H,n}\, \Delta t, \tag{2.3}$$

where L^H is some spatial discretization of the elliptic operator L. In (2.3), $f^{H,n}$ also includes the Dirichlet boundary conditions. With $G(\Omega^H)$ we indicate the space of grid functions that operate on Ω^H; similar notation is used for the other sets. With $w = 0$ and

$$M^H := I - \Delta t\, L^H, \tag{2.4}$$

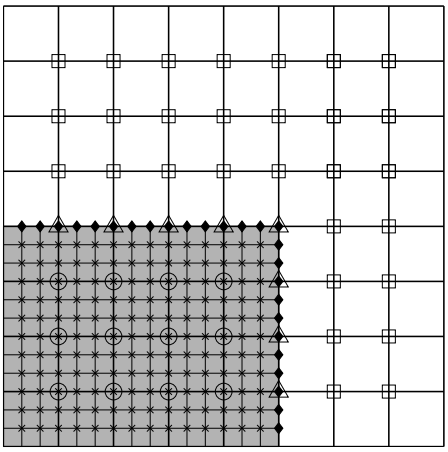

Figure 2: Example of composite grid $\Omega^{H,h}$

we rewrite (2.3) as

$$M^H u_w^{H,n} = u^{H,h,n-1}|_{\Omega^H} + f^{H,n}\,\Delta t. \tag{2.5}$$

We assume $M^H : G(\Omega^H) \to G(\Omega^H)$ to be invertible. We denote by Γ the interface between Ω_l and $\Omega \setminus \Omega_l$. For convenience we partition the coarse grid points as follows

$$\Omega^H = \Omega_l^H \cup \Gamma^H \cup \Omega_c^H, \tag{2.6}$$

where

$$\Omega_l^H := \Omega^H \cap \Omega_l, \qquad \Gamma^H := \Omega^H \cap \Gamma, \qquad \Omega_c^H := \Omega^H \setminus (\Omega_l^H \cup \Gamma^H). \tag{2.7}$$

In Figure 2 the coarse grid points Ω_l^H are marked with circles, while the points Γ^H and Ω_c^H are denoted by triangles and squares respectively. Using the partitioning above, we set

$$u_w^{H,n} =: \begin{pmatrix} u_{l,w}^{H,n} \\ u_{\Gamma,w}^{H,n} \\ u_{c,w}^{H,n} \end{pmatrix}. \tag{2.8}$$

Assuming that the spatial discretization on the coarse grid is such that the stencil at grid point (x, y) involves at most function values at $(x + iH, y + jH)$, with $i, j \in \{-1, 0, 1\}$, we can rewrite (2.5) as

$$\begin{pmatrix} M_l^H & B_{l,\Gamma}^H & 0 \\ B_{\Gamma,l}^H & M_\Gamma^H & B_{\Gamma,c}^H \\ 0 & B_{c,\Gamma}^H & M_c^H \end{pmatrix} \begin{pmatrix} u_{l,w}^{H,n} \\ u_{\Gamma,w}^{H,n} \\ u_{c,w}^{H,n} \end{pmatrix} = \begin{pmatrix} u^{H,h,n-1}|_{\Omega_l^H} \\ u^{H,h,n-1}|_{\Gamma^H} \\ u^{H,h,n-1}|_{\Omega_c^H} \end{pmatrix} + \begin{pmatrix} f_l^{H,n}\,\Delta t \\ f_\Gamma^{H,n}\,\Delta t \\ f_c^{H,n}\,\Delta t \end{pmatrix}. \tag{2.9}$$

The coarse grid solution $u_w^{H,n}$ is used to prescribe artificial boundary conditions on the interface Γ. Boundary conditions on Γ are needed to define a discrete fine grid problem that leads to determining $u_{l,w}^{h,n}$, a local more accurate (both in space and time) approximation of $u(t_n)$. We can prescribe artificial Dirichlet boundary conditions at time t_n by applying an interpolation operator in space $P^{h,H} : G(\Gamma^H) \to G(\Gamma^h)$ to $u_w^{H,n}$; by Γ^h we denoted the set of fine grid points that lie on the interface Γ. In Figure 2 the points Γ^h are marked with small diamonds. If we want to perform time integration with a time step $\delta t = \Delta t/\tau$, we also need to provide boundary conditions on Γ^h at all the intermediate time levels $t_{n-1+k/\tau}$, with $k = 1, 2, \ldots, \tau - 1$. Therefore we perform

linear time interpolation between $u^{H,h,n-1}|_{\Gamma^h}$ and $P^{h,H}u_w^{H,n}$. We let L_l^h be a local fine grid discretization of the operator L and we introduce

$$M_l^h := I - \delta t\, L_l^h. \tag{2.10}$$

A first fine grid approximation ($w = 0$) at time t_n can thus be computed solving

$$\begin{aligned} M_l^h u_{l,w}^{h,n-1+k/\tau} &= u_{l,w}^{h,n-1+(k-1)/\tau} + f_l^{h,n-1+k/\tau}\,\delta t \\ &\quad - B_{l,\Gamma}^h \left(\frac{k}{\tau} P^{h,H} u_{\Gamma,w}^{H,n} + \frac{\tau - k}{\tau} u^{H,h,n-1}|_{\Gamma^h} \right), \qquad \text{for } k = 1, 2, \ldots, \tau. \end{aligned} \tag{2.11}$$

The procedure (2.11) is initialized using

$$u_{l,w}^{h,n-1} = u^{H,h,n-1}|_{\Omega_l^h}. \tag{2.12}$$

We combine all the equations in (2.11) to express $u_{l,w}^{h,n}$ directly in terms of $u^{H,h,n-1}|_{\Omega_l^h}$. We obtain

$$\begin{aligned} \left(M_l^h\right)^\tau u_{l,w}^{h,n} &= u^{H,h,n-1}|_{\Omega_l^h} + \sum_{k=1}^{\tau} \left(M_l^h\right)^{k-1} f_l^{h,n-1+k/\tau}\,\delta t \\ &\quad - \sum_{k=1}^{\tau} \left(M_l^h\right)^{k-1} B_{l,\Gamma}^h \left(\frac{k}{\tau} P^{h,H} u_{\Gamma,w}^{H,n} + \frac{\tau - k}{\tau} u^{H,h,n-1}|_{\Gamma^h} \right), \end{aligned} \tag{2.13}$$

or

$$\left(M_l^h\right)^\tau u_{l,w}^{h,n} = u^{H,h,n-1}|_{\Omega_l^h} + F_l^{h,n}\delta t - W_{l,\Gamma}^n P^{h,H} u_{\Gamma,w}^{H,n} + Z_{l,\Gamma}^n u^{H,h,n-1}|_{\Gamma^h}. \tag{2.14}$$

In (2.14) $F_l^{h,n}$ depends only on the source term and on the fine grid operator M_l^h, while $W_{l,\Gamma}^n$ and $Z_{l,\Gamma}^n$ only depend on M_l^h and $B_{l,\Gamma}^h$.

The fine grid approximation is now used to overall improve the coarse grid solution at time t_n. The fine grid solution is regarded to be more accurate than the coarse grid approximation because it is computed with a grid size $h < H$ and a time step $\delta t \le \Delta t$. The fine grid solution can therefore be used to approximate the local discretization error or defect in Ω_l^H. The defect $\tilde{d}_{l,w-1}^{H,n}$ is estimated plugging the fine grid solution into the coarse grid discretization scheme (cf. the first equation in (2.9))

$$\tilde{d}_{l,w-1}^{H,n} := M_l^H R^{H,h} u_{l,w-1}^{h,n} + B_{l,\Gamma}^H u_{\Gamma,w-1}^{H,n} - u^{H,h,n-1}|_{\Omega_l^H} - f_l^{H,n}\,\Delta t, \tag{2.15}$$

where $R^{H,h} : G(\Omega_l^h) \to G(\Omega_l^H)$ is a restriction operator from the fine to the coarse grid, such that

$$(R^{H,h} u_{l,w-1}^{h,n})(x,y) = u_{l,w-1}^{h,n}(x,y), \quad \forall (x,y) \in \Omega_l^H. \tag{2.16}$$

The defect $\tilde{d}_{l,w-1}^{H,n}$ is now added to the right hand side of (2.9). A more accurate coarse grid approximation can thus be computed solving

$$\begin{aligned} M^H u_w^{H,n} &= \begin{pmatrix} u^{H,h,n-1}|_{\Omega_l^H} \\ u^{H,h,n-1}|_{\Gamma^H} \\ u^{H,h,n-1}|_{\Omega_c^H} \end{pmatrix} + \begin{pmatrix} f_l^{H,n}\,\Delta t + \tilde{d}_{l,w-1}^{H,n} \\ f_\Gamma^{H,n}\,\Delta t \\ f_c^{H,n}\,\Delta t \end{pmatrix} \\ &= \begin{pmatrix} 0 \\ u^{H,h,n-1}|_{\Gamma^H} \\ u^{H,h,n-1}|_{\Omega_c^H} \end{pmatrix} + \begin{pmatrix} M_l^H R^{H,h} u_{l,w-1}^{h,n} + B_{l,\Gamma}^H u_{\Gamma,w-1}^{H,n} \\ f_\Gamma^{H,n}\,\Delta t \\ f_c^{H,n}\,\Delta t \end{pmatrix}. \end{aligned} \tag{2.17}$$

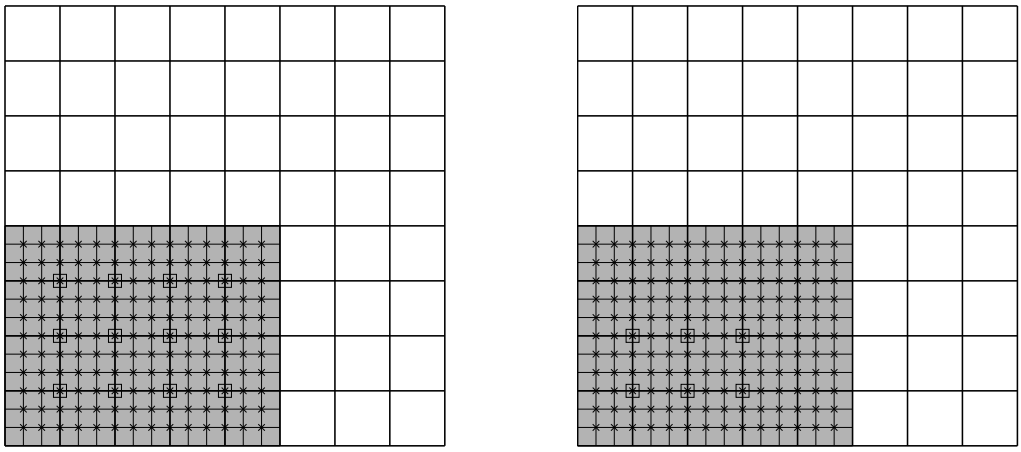

(a) (b)

Figure 3: Composite grid without (a) and with (b) safety region.

The new coarse grid solution can be used to update the boundary conditions for a new local problem on Ω_l^h, which in turn will correct the coarse grid approximation. This defines the LDC iteration process, cf. Figure 1. In [13] it is proved that, if the LDC iteration converges, then the limit solution is such that the coarse and fine solution at t_n coincide in Ω_l^H, the common points between coarse and fine grid.

We note that previous results [3, 7, 12, 23] for the stationary case show that it may be beneficial to compute $\tilde{d}_{l,w-1}^{H,n}$ not at all points of Ω_l^H, but in a subset Ω_{def}^H only. In particular, points lying close to the interface Γ should be excluded. In this way points of Γ and points of Ω_{def}^H are separated by a so called safety region. Figure 3 shows an example of a composite grid without a safety region (a) and with a safety region (b). In the figure, points Ω_{def}^H are marked with a square. With the introduction of the safety region, we can rewrite (2.17) as

$$M^H u_w^{H,n} = \begin{pmatrix} 0 \\ u^{H,h,n-1}|_{\Gamma^H} \\ u^{H,h,n-1}|_{\Omega_c^H} \end{pmatrix} + \begin{pmatrix} (I - X_l^H) f_l^{H,n} + X_l^H (M_l^H R^{H,h} u_{l,w-1}^{h,n} + B_{l,\Gamma}^H u_{\Gamma,w-1}^{H,n}) \\ f_\Gamma^{H,n} \Delta t \\ f_c^{H,n} \Delta t, \end{pmatrix}, \tag{2.18}$$

where the operator $X_l^H : G(\Omega_l^H) \to G(\Omega_l^H)$ is defined by

$$\left(X_l^H u_l^{H,n}\right)(x,y) := \begin{cases} u_l^{H,n}(x,y), & (x,y) \in \Omega_{def}^H, \\ 0, & (x,y) \in \Omega_l^H \setminus \Omega_{def}^H. \end{cases} \tag{2.19}$$

In the next section we find an expression for the LDC iteration matrix that describes the LDC iteration at time t_n.

3 The iteration matrix

In order to find an expression for the matrix that describes the LDC iteration at time t_n, we follow a similar approach as done in [3] for stationary problems. In [3] the LDC iteration is expressed in terms of the iteration that takes place on Γ^H only and it is shown that, if the iteration on Γ^H converges, then the entire LDC iteration

converges; the set Γ^H, see its definition in (2.7), includes the coarse grid points that lie on the interface between coarse and fine grid. Previously, other approaches were proposed. In [12] the LDC iteration for elliptic problems is expressed in terms of grid functions that operate on Γ^h, i.e. the set of fine grid points on the interface. In [8], with reference to boundary value problems, the LDC iteration that takes place on the whole set of composite grid points is considered.

Combination of (2.15) and (2.18) yields

$$\begin{aligned}
&\begin{pmatrix} (M_l^h)^\tau & 0 & W_{l,\Gamma}^n P^{h,H} & 0 \\ 0 & M_l^H & B_{l,\Gamma}^H & 0 \\ 0 & B_{\Gamma,l}^H & M_\Gamma^H & B_{\Gamma,c}^H \\ 0 & 0 & B_{c,\Gamma}^H & M_c^H \end{pmatrix} \begin{pmatrix} u_{l,w}^{h,n} \\ u_{l,w}^{H,n} \\ u_{\Gamma,w}^{H,n} \\ u_{c,w}^{H,n} \end{pmatrix} \\
&\quad = \begin{pmatrix} 0 & 0 & 0 & 0 \\ X_l^H M_l^H R^{H,h} & 0 & X_l^H B_{l,\Gamma}^H & 0 \\ 0 & 0 & 0 & 0 \\ 0 & 0 & 0 & 0 \end{pmatrix} \begin{pmatrix} u_{l,w-1}^{h,n} \\ u_{l,w-1}^{H,n} \\ u_{\Gamma,w-1}^{H,n} \\ u_{c,w-1}^{H,n} \end{pmatrix} + \begin{pmatrix} u^{H,h,n-1}|_{\Omega_l^h} \\ (I - X_l^H) u^{H,h,n-1}|_{\Omega_l^H} \\ u^{H,h,n-1}|_{\Gamma_H} \\ u^{H,h,n-1}|_{\Omega_c^H} \end{pmatrix} \\
&\qquad + \begin{pmatrix} F_l^{h,n} \Delta t \\ (I - X_l^H) f_l^{H,n} \\ f_\Gamma^{H,n} \delta t \\ f_c^{H,n} \delta t \end{pmatrix} + \begin{pmatrix} Z_{l,\Gamma}^n u^{H,h,n-1}|_{\Gamma^h} \\ 0 \\ 0 \\ 0 \end{pmatrix}, \qquad (3.1)
\end{aligned}$$

which can also be expressed using the short notation

$$M^{H,h} u_w^{H,h,n} = S^{H,h} u_{w-1}^{H,h,n} + \tilde{u}^{H,h,n-1} + \tilde{f}^{H,h,n} + \tilde{z}^{H,h,n-1}. \qquad (3.2)$$

The limit of the LDC iteration at time t_n is indicated by

$$u^{H,h,n} := \begin{pmatrix} u_l^{h,n} \\ u_l^{H,n} \\ u_\Gamma^{H,n} \\ u_c^{H,n} \end{pmatrix}. \qquad (3.3)$$

In (3.3) we removed the subscript w that numbers the LDC iterations. Since $u^{H,h,n}$ is the fixed point, one has

$$M^{H,h} u^{H,h,n} = S^{H,h} u^{H,h,n} + \tilde{u}^{H,h,n-1} + \tilde{f}^{H,h,n} + \tilde{z}^{H,h,n-1}. \qquad (3.4)$$

If we introduce the iteration error of the LDC method by

$$e_w^{H,h,n} := u_w^{H,h,n} - u^{H,h,n}, \qquad (3.5)$$

and we subtract (3.2) and (3.4), we can write the expression for successive iteration errors

$$M^{H,h} e_w^{H,h,n} = S^{H,h} e_{w-1}^{H,h,n}. \qquad (3.6)$$

Note that the convergence of the LDC method does not depend on the source term, on the Dirichlet boundary conditions and on the solution at the previous time step. Definitions of $M^{H,h}$ and $S^{H,h}$ enables us to rewrite (3.6) as

$$\begin{pmatrix} (M_l^h)^\tau & 0 & W_{l,\Gamma}^n & 0 \\ 0 & M_l^H & B_{l,\Gamma}^H & 0 \\ 0 & B_{\Gamma,l}^H & M_\Gamma^H & B_{\Gamma,c}^H \\ 0 & 0 & B_{c,\Gamma}^H & M_c^H \end{pmatrix} \begin{pmatrix} e_{l,w}^{h,n} \\ e_{l,w}^{H,n} \\ e_{\Gamma,w}^{H,n} \\ e_{c,w}^{H,n} \end{pmatrix} = \begin{pmatrix} 0 \\ X_l^H M_l^H R^{H,h} e_{l,w-1}^{h,n} + X_l^H B_{l,\Gamma}^H e_{\Gamma,w-1}^{H,n} \\ 0 \\ 0 \end{pmatrix}. \qquad (3.7)$$

The first equation of this system yields

$$e_{l,w}^{h,n} = -\left((M_l^h)^\tau\right)^{-1} W_{l,\Gamma}^n e_{\Gamma,w}^{H,n}. \tag{3.8}$$

Replacing w with $w-1$ in (3.8), we can reformulate system (3.7) as

$$\begin{pmatrix} M_l^H & B_{l,\Gamma}^H & 0 \\ B_{\Gamma,l}^H & M_\Gamma^H & B_{\Gamma,c}^H \\ 0 & B_{c,\Gamma}^H & M_c^H \end{pmatrix} \begin{pmatrix} e_{l,w}^{H,n} \\ e_{\Gamma,w}^{H,n} \\ e_{c,w}^{H,n} \end{pmatrix}$$

$$= \begin{pmatrix} -X_l^H M_l^H R^{H,h}\left((M_l^h)^\tau\right)^{-1} W_{l,\Gamma}^n e_{\Gamma,w-1}^{H,n} + X_l^H B_{l,\Gamma}^H e_{\Gamma,w-1}^{H,n} \\ 0 \\ 0 \end{pmatrix}, \tag{3.9}$$

or, equivalently,

$$M^H e_w^{H,n} = \begin{pmatrix} I \\ 0 \\ 0 \end{pmatrix} X_l^H \left(B_{l,\Gamma}^H - M_l^H R^{H,h}\left((M_l^h)^\tau\right)^{-1} W_{l,\Gamma}^n \right) e_{\Gamma,w-1}^{H,n}. \tag{3.10}$$

This leads to the following theorem.

Theorem 3.1
Consider the following iteration that takes place on the interface only:

$$e_{\Gamma,w}^{H,n} = M_{iter}\, e_{\Gamma,w-1}^{H,n}, \qquad w = 1, 2, \ldots \tag{3.11}$$

in which the iteration matrix $M_{iter} : G(\Gamma^H) \to G(\Gamma^H)$ *is defined by*

$$M_{iter} := \begin{pmatrix} 0 & I & 0 \end{pmatrix} (M^H)^{-1} \begin{pmatrix} I \\ 0 \\ 0 \end{pmatrix} X_l^H \left(B_{l,\Gamma}^H - M_l^H R^{H,h}\left((M_l^h)^\tau\right)^{-1} W_{l,\Gamma}^n \right). \tag{3.12}$$

If iteration (3.11) *converges, then the LDC iteration converges.*

Proof. It is easy to verify that (3.10) gives (3.11). Equation (3.11) describes the behavior of the component $e_{\Gamma,w}^H$ of the iteration error; the other components can be expressed in terms of $e_{\Gamma,w}^H$ by (3.8) and (3.10). Equations (3.8) and (3.10) show that if $e_{\Gamma,w}^H \to 0$ $(w \to \infty)$, also $e_w^H \to 0$ $(w \to \infty)$. □

Theorem 3.1 is the time-dependent equivalent of [3, Theorem 2]. Theorem 3.1 states that, if the iteration that takes place on the interface Γ^H at time t_n converges, then the entire LDC iteration at time t_n converges to a fixed point. This means that for proving convergence of the LDC method for parabolic problems, it is sufficient to show that the spectral radius of the matrix M_{iter} is less than one. This is true if $\|M_{iter}\|_\infty < 1$. Following the same approach as in [3], we split the iteration matrix M_{iter} according to

$$M_{iter} = M_1 M_2, \tag{3.13}$$

where $M_1 : G(\Omega_l^H) \to G(\Gamma^H)$ is expressed by

$$M_1 = \begin{pmatrix} 0 & I & 0 \end{pmatrix} (M^H)^{-1} \begin{pmatrix} I \\ 0 \\ 0 \end{pmatrix}, \tag{3.14}$$

and $M_2 : G(\Gamma^H) \to G(\Omega_l^H)$ by

$$M_2 = X_l^H \left(B_{l,\Gamma}^H - M_l^H R^{H,h} \left((M_l^h)^\tau \right)^{-1} W_{l,\Gamma}^n \right). \tag{3.15}$$

In the next section we introduce a one-dimensional model problem. For such a problem and for a particular choice of the grids and the discretization schemes, the properties of M_{iter} can be studied analytically.

4 A one-dimensional model problem

We consider the application of the LDC method to the solution of the one-dimensional heat equation

$$\begin{cases} \dfrac{\partial u(x,t)}{\partial t} = \dfrac{\partial^2 u(x,t)}{\partial x^2} + f(x,t), & \text{in } \Omega = (0,1), \text{ for } t > 0, \\ u(0,t) = \psi_{\text{left}}(t), & \text{for } t > 0, \\ u(1,t) = \psi_{\text{right}}(t), & \text{for } t > 0, \\ u(x,0) = \varphi_0(x), & \text{in } \bar{\Omega} = [0,1], \end{cases} \tag{4.1}$$

where $f(x,t)$, $\psi_{\text{left}}(t)$, $\psi_{\text{right}}(t)$ and $\varphi_0(x)$ are given functions. With reference to problem (4.1), we study the convergence behavior of the LDC method at a generic time step t_n. The LDC method is applied with the following settings: the global uniform grid has grid size $H = 1/N$ (N integer and $N > 1$) and grid points

$$\Omega^H = \{iH \mid i = 1, 2, \ldots, N-1\}. \tag{4.2}$$

On Ω^H we perform spatial discretization by finite differences; in particular, we adopt the standard three-point centered differences scheme to approximate $\partial^2/\partial x^2$. The temporal discretization is performed by the Euler backward scheme with a time step Δt. In this way the coarse grid operator M^H is expressed by

$$M^H = I - \Delta t\, L^H = I - \frac{\Delta t}{H^2} \begin{pmatrix} \ddots & \ddots & \ddots & & \\ & 1 & -2 & 1 & \\ & & \ddots & \ddots & \ddots \end{pmatrix}. \tag{4.3}$$

We let the local region be $\Omega_l = (0, \gamma)$, with γ a multiple of H such that $0 < \gamma < 1$. In our analysis we will replace the discrete operator M_l^h by the continuous operator

$$M := \frac{\partial}{\partial t} - \frac{\partial^2}{\partial x^2}. \tag{4.4}$$

This corresponds to letting $h \to 0$ and $\delta t \to 0$. This is done for analysis purposes only; in practice one will always have $h > 0$ and $\delta t > 0$. However, the results presented in [1] for stationary diffusion problems and the numerical experiments in Section 6 of this paper support this approach. In [1] the LDC iteration matrix is studied both for a continuous ($h = 0$) and for a discrete local problem ($h > 0$): the two approaches lead to the same conclusions. Note that in our one-dimensional setting the space interpolation operator $P^{H,h}$ reduces to the identity function. Also note that, in 1D and with $\Omega_l = (0, \gamma)$, the set Γ^H reduces to one point. As a consequence, the two operators M_1 and M_2

turn out to be a row and a column vector respectively, while M_{iter} is their inner product, so a real number. In this context, when writing $\|M_1\|_\infty$ or $\|M_2\|_\infty$ we will therefore mean the standard vector infinity norm, while $\|M_{\text{iter}}\|_\infty$ is the absolute value of the real number M_{iter}. For the model problem illustrated here, we will determine bounds for $\|M_1\|_\infty$ in Section 4.1 and an expression for M_2 in Section 4.2. Before that we emphasize the fact that, in our analysis, we will always assume γ to be a given multiple of H such that $0 < \gamma < 1$. The special cases $\gamma = 0$ and $\gamma = 1$ are of minor interest: if $\gamma = 0$, the local region Ω_l reduces to the left boundary point and we have no defect, while the case $\gamma = 1$ is not interesting because Ω_l coincides with the global domain.

4.1 Bounds for the M_1 infinity norm

In this section we consider the operator M_1 as defined in (3.14), with M^H given by (4.3). It is easy to verify that

$$\|M_1\|_\infty \leq \|(M^H)^{-1}\|_\infty. \tag{4.5}$$

Lemma 4.1 provides a first bound for the infinity norm of $(M^H)^{-1}$.

Lemma 4.1
With M^H given by (4.3)*, the following bound for $\|(M^H)^{-1}\|_\infty$ holds*

$$\|(M^H)^{-1}\|_\infty \leq 1. \tag{4.6}$$

Proof. We express M^H as

$$M^H = I - \Delta t\, L^H = (1 + 2d)(I + B), \tag{4.7}$$

where the scalar $d \geq 0$ and the matrix B are given by

$$d = \frac{\Delta t}{H^2}, \qquad B = \begin{pmatrix} \ddots & \ddots & \ddots & & \\ & \frac{-d}{1+2d} & 0 & \frac{-d}{1+2d} & \\ & & \ddots & \ddots & \ddots \end{pmatrix}. \tag{4.8}$$

It is easy to verify that

$$\|B\|_\infty = \frac{2d}{1+2d} < 1. \tag{4.9}$$

We write

$$(I + B)^{-1} = I - B + B^2 - B^3 + \cdots \tag{4.10}$$

and

$$\|(I + B)^{-1}\|_\infty \leq \|I\|_\infty + \|B\|_\infty + \|B\|_\infty^2 + \|B\|_\infty^3 + \cdots \leq \frac{1}{1 - \|B\|_\infty} = 1 + 2d. \tag{4.11}$$

Since

$$\|(M^H)^{-1}\|_\infty = \|(I - \Delta t L^H)^{-1}\|_\infty = \frac{1}{1+2d}\|(I + B)^{-1}\|_\infty, \tag{4.12}$$

we deduce

$$\|(M^H)^{-1}\|_\infty \leq 1. \tag{4.13}$$

□

A second bound for the infinity norm of $(M^H)^{-1}$ is the result of Lemma 4.2.

Lemma 4.2
With M^H *given by* (4.3)*, the following bound for* $\|(M^H)^{-1}\|_\infty$ *holds*

$$\|(M^H)^{-1}\|_\infty \leq \frac{1}{\Delta t}. \tag{4.14}$$

Proof. Since matrix $M^H \in \mathbb{R}^{N-1,N-1}$ is symmetric, for the Symmetric Diagonalization Theorem, see for example [17, Theorem 4 at page 458], it can be written as

$$M^H = Q\, D\, Q^T, \tag{4.15}$$

where $Q \in \mathbb{R}^{N-1,N-1}$ is orthogonal and $D \in \mathbb{R}^{N-1,N-1}$ is diagonal. The diagonal entries of D are

$$d_j = 1 + 4\frac{\Delta t}{H^2}\sin^2(j\pi H/2), \quad j = 1, 2, \ldots, N-1, \tag{4.16}$$

and they coincide with the eigenvalues of M^H. Note that the smallest eigenvalue is d_1. The orthogonal matrix Q has entries q_{ij} given by

$$q_{ij} = \sqrt{2H}\,\sin(i\,j\,\pi H), \quad i, j = 1, 2, \ldots, N-1. \tag{4.17}$$

From (4.17) we note that Q is also symmetric. We can thus write

$$(M^H)^{-1} = Q\, D^{-1}\, Q. \tag{4.18}$$

It can easily be shown that

$$\|Q\|_\infty = \max_i \left\{ \sum_{j=1}^{N-1} |q_{ij}| \right\} \leq (N-1)\sqrt{2H}, \tag{4.19}$$

$$\|D^{-1}Q\|_\infty = \max_i \left\{ \frac{1}{d_i} \sum_{j=1}^{N-1} |q_{ij}| \right\} \leq (N-1)\sqrt{2H}\,\frac{1}{d_1}. \tag{4.20}$$

We note that, since we chose the integer $N > 1$, then $H = 1/N$ is such that $0 \leq H \leq 1/2$. Using the following inequality

$$\sin^2\left(\frac{\pi H}{2}\right) \leq H, \quad \text{for } 0 \leq H \leq 1/2, \tag{4.21}$$

we can show that

$$\frac{1}{d_1} = \frac{1}{1 + 4\Delta t/H^2 \sin^2(\pi H/2)} \leq \frac{1}{1 + 4\Delta t/H} \leq \frac{H}{4\Delta t}. \tag{4.22}$$

Combination of (4.18), (4.19), (4.20) and (4.22) finally yields

$$\|(M^H)^{-1}\|_\infty \leq \|Q\|_\infty \, \|D^{-1}Q\|_\infty \leq (N-1)^2 2H^2 \frac{1}{4\Delta t} \leq \frac{1}{\Delta t}. \tag{4.23}$$

□

Results of Lemma 4.1 and Lemma 4.2 are illustrated in Figure 4, where $\|(M^H)^{-1}\|_\infty$ is plotted as a function of Δt for two different values of the grid size H. Formula (4.5) and the results of Lemma 4.1 and Lemma 4.2 are combined in Theorem 4.3.

Theorem 4.3
The following bound for $\|M_1\|_\infty$ *holds*

$$\|M_1\|_\infty \leq \min(1, \frac{1}{\Delta t}). \tag{4.24}$$

Note that the bound provided by Theorem 4.3 is independent of H and thus it holds for any choice of the coarse grid size.

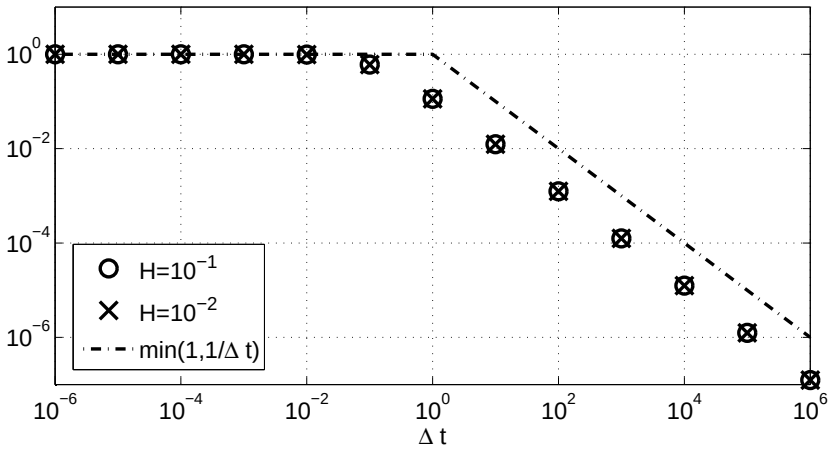

Figure 4: Plot of $\|(M^H)^{-1}\|_\infty$, with M^H defined by (4.3), as a function of Δt for two values of the grid size H and plot of the bounds provided by Lemma 4.1 and Lemma 4.2.

4.2 The expression of the M_2 infinity norm

In this section we find an expression for the infinity norm of M_2. We let $g_\Gamma^{H,n} \in \mathbb{R}$ be the solution found at point $x = \gamma$ by performing one time step Δt on the coarse grid. From the definition of M_2, see (3.15), we have that

$$M_2 g_\Gamma^{H,n} = X_l^H \left(B_{l,\Gamma}^H g_\Gamma^{H,n} + M_l^H R^{H,h} u^n \right), \tag{4.25}$$

where

$$u^n = -\left((M_l^h)^\tau \right)^{-1} W_{l,\Gamma}^n g_\Gamma^{H,n}. \tag{4.26}$$

In view of (2.14) and the assumptions we made on $(M_l^h)^\tau$, it follows that u^n is the solution of the one-dimensional heat equation

$$\begin{cases} \dfrac{\partial u(x,t)}{\partial t} = \dfrac{\partial^2 u(x,t)}{\partial x^2}, & \text{for } x \in (0,\gamma),\ t \in (0,\Delta t], \\ u(0,t) = 0, & \text{for } t \in (0,\Delta t], \\ u(\gamma,t) = g_\Gamma^{H,n} \dfrac{t}{\Delta t}, & \text{for } t \in (0,\Delta t], \\ u(x,0) = 0, & \text{for } x \in [0,\gamma]. \end{cases} \tag{4.27}$$

In order to find an expression for M_2, we want to find the exact analytical solution of problem (4.27). For that purpose we introduce the auxiliary function

$$v(x,t) := u(x,t) - g_\Gamma^{H,n} \left(\frac{1}{6\gamma\Delta t} x^3 - \frac{\gamma}{6\Delta t} x + \frac{xt}{\gamma\Delta t} \right). \tag{4.28}$$

Combination of (4.27) and (4.28) shows that v satisfies

$$\begin{cases} \dfrac{\partial v(x,t)}{\partial t} = \dfrac{\partial^2 v(x,t)}{\partial x^2}, & \text{for } x \in (0,\gamma),\ t \in (0,\Delta t], \\ v(0,t) = v(\gamma,t) = 0, & \text{for } t \in (0,\Delta t], \\ v(x,0) = -\dfrac{g_\Gamma^{H,n}}{6\gamma\Delta t} x^3 + \dfrac{g_\Gamma^{H,n}\gamma}{6\Delta t} x, & \text{for } x \in [0,\gamma]. \end{cases} \tag{4.29}$$

Problem (4.29) can be solved using the technique of separation of variables. We express its solution in the form

$$v(x,t) = \frac{g_\Gamma^{H,n}}{\Delta t} \sum_{m=1}^{\infty} v_m e^{-m^2\pi^2 t/\gamma^2} \sin\left(\frac{m\pi x}{\gamma}\right), \tag{4.30}$$

where the coefficients v_m are to be computed from the initial condition

$$v(x,0) = \frac{g_\Gamma^{H,n}}{\Delta t} \sum_{m=1}^{\infty} v_m \sin\left(\frac{m\pi x}{\gamma}\right) = -\frac{g_\Gamma^{H,n}}{6\gamma\Delta t}x^3 + \frac{g_\Gamma^{H,n}\gamma}{6\Delta t}x. \tag{4.31}$$

We find

$$v_m = \frac{2}{\gamma}\frac{\Delta t}{g_\Gamma^{H,n}} \int_0^\gamma v(x,0)\,dx = -\frac{2(-1)^m\gamma^2}{m^3\pi^3}. \tag{4.32}$$

Using (4.30), the solution of the original problem (4.27) turns out to be

$$u(x,t) = \frac{g_\Gamma^{H,n}}{\Delta t}\left(\sum_{m=1}^{\infty} v_m e^{-m^2\pi^2 t/\gamma^2} \sin\left(\frac{m\pi x}{\gamma}\right) + \frac{1}{6\gamma}x^3 - \frac{\gamma}{6}x + \frac{xt}{\gamma}\right). \tag{4.33}$$

The solution $u(x,t)$ is now used to express the product $M_2 g_\Gamma^{H,n}$. Equation (4.25) states that $M_2 g_\Gamma^{H,n}$ equals the residual of the coarse grid discretization scheme (centered differences and implicit Euler) applied to the function $u(x,t)$ for all grid points $x \in \Omega_{\text{def}}^H$. Taking already in account that $u(x,0) = 0$, we have

$$M_2 g_\Gamma^{H,n}(x) = u(x,\Delta t) - \frac{\Delta t}{H^2}\left(u(x+H,\Delta t) - 2u(x,\Delta t) + u(x-H,\Delta t)\right). \tag{4.34}$$

We use the identity

$$\begin{aligned} \sin\left(\frac{m\pi(x+H)}{\gamma}\right) - 2\sin\left(\frac{m\pi x}{\gamma}\right) + \sin\left(\frac{m\pi(x-H)}{\gamma}\right) \\ = -4\sin\left(\frac{m\pi H}{2\gamma}\right)\sin\left(\frac{m\pi x}{\gamma}\right) \end{aligned} \tag{4.35}$$

to combine (4.33) and (4.34) into

$$\begin{aligned} M_2 g_\Gamma^{H,n}(x) =& \frac{g_\Gamma^{H,n}}{\Delta t}\left(\sum_{m=1}^{\infty} v_m e^{-m^2\pi^2\Delta t/\gamma^2} \sin\left(\frac{m\pi x}{\gamma}\right) + \frac{1}{6\gamma}x^3 - \frac{\gamma}{6}x\right) \\ &+ \frac{4g_\Gamma^{H,n}}{H^2} \sum_{m=1}^{\infty} v_m e^{-m^2\pi^2\Delta t/\gamma^2} \sin\left(\frac{m\pi H}{2\gamma}\right)\sin\left(\frac{m\pi x}{\gamma}\right). \end{aligned} \tag{4.36}$$

Assuming that the function u is sufficiently smooth, another expression for $M_2 g_\Gamma^{H,n}(x)$ can be derived using Taylor expansions on the right hand side of (4.34) and the fact that u satisfies the partial differential equation in (4.27). We obtain

$$M_2 g_\Gamma^{H,n}(x) = \frac{1}{2}\frac{\partial^2 u}{\partial t^2}\Big|_{(x,\vartheta)} \Delta t^2 + \frac{1}{12}\frac{\partial^4 u}{\partial x^4}\Big|_{(\xi,\Delta t)} \Delta t\, H^2, \tag{4.37}$$

with $x - H < \xi < x + H$ and $0 < \vartheta < \Delta t$. The time and spatial derivatives of u can be computed differentiating term by term the series in (4.33). A sufficient condition for this is that the resulting series are absolute convergent. We obtain

$$\frac{\partial^2 u}{\partial t^2}\Big|_{(x,\vartheta)} = \frac{g_\Gamma^{H,n}}{\Delta t}\frac{2\pi}{\gamma^2} \sum_{m=1}^{\infty} (-1)^m\, m\, e^{-m^2\pi^2\vartheta/\gamma^2} \sin\left(\frac{m\pi x}{\gamma}\right), \tag{4.38}$$

$$\frac{\partial^4 u}{\partial x^4}\Big|_{(\xi,\Delta t)} = \frac{g_\Gamma^{H,n}}{\Delta t}\frac{2\pi}{\gamma^2} \sum_{m=1}^{\infty} (-1)^m\, m\, e^{-m^2\pi^2\Delta t/\gamma^2} \sin\left(\frac{m\pi\xi}{\gamma}\right). \tag{4.39}$$

Clearly the series on the right hand side of (4.38) and (4.39) are absolute convergent for any positive Δt and ϑ.

5 Iteration matrix norm asymptotics

With reference to the one-dimensional heat equation (4.1) and the settings illustrated in Section 4, in Section 5.1 we study the asymptotic expression of $\|M_{iter}\|_\infty$ for $\Delta t \downarrow 0$, while in Section 5.2 we deal with M_{iter} when $\Delta t \to +\infty$. The limit case $\Delta t \to +\infty$ corresponds to the stationary case limit; this is of interest in practical applications when a time-dependent problem is solved to compute a stationary solution.

5.1 The asymptotic behavior of $\|M_{iter}\|_\infty$ for $\Delta t \downarrow 0$

Combination of (3.13) with the result of Theorem 4.3 yields

$$\|M_{iter}\|_\infty \leq \|M_1\|_\infty \|M_2\|_\infty \leq \|M_2\|_\infty, \quad \text{for } \Delta t < 1. \tag{5.1}$$

As a consequence, in our analysis for $\Delta t \downarrow 0$ we will only consider the infinity norm of M_2. In particular, we will focus on the expression for M_2 as given by (4.37).

In the perspective of studying $\|M_2\|_\infty$ for $\Delta t \ll 1$, we first solve a preliminary problem. We introduce the following series (cf. (4.38) and (4.39))

$$S_x(\vartheta) := \sum_{m=1}^{\infty} (-1)^m s_m \sin\Big(\frac{m\pi x}{\gamma}\Big), \tag{5.2}$$

where

$$s_m := m\, e^{-m^2\vartheta}, \tag{5.3}$$

and we study the asymptotic behavior of $S_x(\vartheta)$ for $\vartheta \downarrow 0$ and fixed $0 < x < \gamma$. Using the fact that $s_{-m} = s_m$ for all integers m, we rewrite (5.2) as

$$S_x(\vartheta) = -\frac{1}{2i} \sum_{m=-\infty}^{+\infty} m\, e^{-m^2\vartheta}\, e^{-im\pi(x/\gamma - 1)}. \tag{5.4}$$

If a function $f(y)$ is sufficiently smooth, the following relation, which is known in the literature (cf. for instance [19]) as Poisson summation formula, holds:

$$\sum_{m=-\infty}^{+\infty} f(m) e^{-im\omega} = \sum_{k=-\infty}^{+\infty} \hat{f}(\omega + 2\pi k). \tag{5.5}$$

The term $\hat{f}$ which appears in (5.5) is the Fourier transform of $f(y)$, defined by

$$\hat{f}(\omega) := \int_{-\infty}^{+\infty} f(y)\, e^{-iy\omega}\, dy. \tag{5.6}$$

For

$$f(y) = y\, e^{-y^2\vartheta}, \tag{5.7}$$

we have

$$\hat{f}(\omega) = -i\, \frac{\pi^{1/2}}{2\,\vartheta^{3/2}}\, \omega\, e^{-\omega^2/(4\vartheta)}. \tag{5.8}$$

Using Poisson summation formula, we can thus rewrite (5.4) as

$$S_x(\vartheta) = \frac{\pi^{3/2}}{4\,\vartheta^{3/2}} \sum_{k=-\infty}^{+\infty} \Big(\frac{x}{\gamma} - 1 + 2k\Big) \exp\Big(-\frac{\pi^2(x/\gamma - 1 + 2k)^2}{4\vartheta}\Big). \tag{5.9}$$

If we introduce the new variables

$$y := \frac{1}{2}\left(1 - \frac{x}{\gamma}\right), \quad \alpha := \frac{\pi^2}{\vartheta}, \tag{5.10}$$

the original problem for $S_x(\vartheta)$ can be reformulated as follows: study the asymptotics of

$$T_y(\alpha) := -\frac{\alpha^{3/2}}{2\pi^{3/2}} \sum_{k=-\infty}^{+\infty} (k-y)\, e^{-\alpha(k-y)^2} \tag{5.11}$$

for $\alpha \to +\infty$ and $0 < y < 1/2$. For that, we need the results of the following lemma.

Lemma 5.1
The following identity holds:

$$\lim_{\alpha\to+\infty} \alpha \sum_{k=1}^{+\infty} k^2\, e^{-k\alpha\beta} = 0, \qquad \beta > 0. \tag{5.12}$$

Proof. Note that by assumption β is positive. Starting from the identity

$$\sum_{k=1}^{+\infty} e^{-k\alpha\beta} = \frac{e^{-\alpha\beta}}{1 - e^{-\alpha\beta}}, \qquad \alpha > 0, \tag{5.13}$$

it can be easily shown that

$$\alpha \sum_{k=1}^{+\infty} k^2\, e^{-k\alpha\beta} = \alpha\, \frac{e^{-\alpha\beta}(1 + e^{-\alpha\beta})}{(1 - e^{-\alpha\beta})^3}, \qquad \alpha > 0. \tag{5.14}$$

Claim (5.12) follows immediately since the limit for $\alpha \to +\infty$ of the right hand side of (5.14) is 0. □

The result of Lemma 5.1 is used in the proof of Theorem 5.2, which provides the asymptotic expression of $T_y(\alpha)$ for $\alpha \to +\infty$. First we introduce the following notation: we say that $f(\alpha)$ is asymptotically equivalent to $g(\alpha)$ for $\alpha \to \alpha_0$ and we write

$$f(\alpha) \approx g(\alpha), \qquad (\alpha \to \alpha_0), \tag{5.15}$$

if

$$\lim_{\alpha\to\alpha_0} \frac{f(\alpha)}{g(\alpha)} = 1. \tag{5.16}$$

Theorem 5.2
The following equivalence holds:

$$T_y(\alpha) \approx \frac{1}{2\pi^{3/2}}\, \alpha^{3/2}\, y\, e^{-\alpha y^2}, \qquad (\alpha \to +\infty), \tag{5.17}$$

with $0 < y < 1/2$.

Proof. For proving (5.17) it is sufficient to show (cf. (5.11)) that

$$\lim_{\alpha\to+\infty} \frac{1}{y e^{-\alpha y^2}} \sum_{k=-\infty}^{+\infty} (k-y) e^{-\alpha(k-y)^2} = -1, \qquad \text{with } 0 < y < 1/2. \tag{5.18}$$

The series in (5.18) can be written in a more convenient way as follows:

$$\begin{aligned}\sum_{k=-\infty}^{+\infty}(k-y)e^{-\alpha(k-y)^2} &= -ye^{-\alpha y^2}+\sum_{k=1}^{+\infty}\left((k-y)e^{-\alpha(k-y)^2}-(k+y)e^{-\alpha(k+y)^2}\right)\\ &= -ye^{-\alpha y^2}-y\sum_{k=1}^{+\infty}\left(e^{-\alpha(k-y)^2}+e^{-\alpha(k+y)^2}\right)+\sum_{k=1}^{+\infty}k\left(e^{-\alpha(k-y)^2}-e^{-\alpha(k+y)^2}\right)\\ &= -ye^{-\alpha y^2}\left(1+\sum_{k=1}^{+\infty}e^{-\alpha k^2}\left(e^{2\alpha ky}+e^{-2\alpha ky}\right)-\frac{1}{y}\sum_{k=1}^{+\infty}k\,e^{-\alpha k^2}\left(e^{2\alpha ky}-e^{-2\alpha ky}\right)\right).\end{aligned} \tag{5.19}$$

We proceed showing that

$$\lim_{\alpha\to\infty}\sum_{k=1}^{+\infty}e^{-\alpha k^2}\left(e^{2\alpha ky}+e^{-2\alpha ky}\right)=0,\qquad 0<y<1/2, \tag{5.20}$$

and

$$\lim_{\alpha\to\infty}\frac{1}{y}\sum_{k=1}^{+\infty}k\,e^{-\alpha k^2}\left(e^{2\alpha ky}-e^{-2\alpha ky}\right)=0,\qquad 0<y<1/2. \tag{5.21}$$

We start from (5.20). We notice that all the terms of the series in (5.20) are positive. The idea is thus to find an upper bound for the sum of the series which goes to 0 as $\alpha\to+\infty$. We write

$$\begin{aligned}0\le\sum_{k=1}^{+\infty}e^{-\alpha k^2}\left(e^{2\alpha ky}+e^{-2\alpha ky}\right)&\le 2\sum_{k=1}^{+\infty}e^{-\alpha k^2}e^{2\alpha ky}\le 2\sum_{k=1}^{+\infty}e^{-\alpha k}e^{2\alpha ky}\\ &=2\sum_{k=1}^{+\infty}\left(e^{-\alpha(1-2y)}\right)^k\le 2\,\frac{e^{-\alpha(1-2y)}}{1-e^{-\alpha(1-2y)}}.\end{aligned} \tag{5.22}$$

Clearly, if $0<y<1/2$, the last term in (5.22) goes to 0 for $\alpha\to+\infty$. This proves (5.20).

We adopt a similar strategy for (5.21). Also in this case we deal with a series with positive terms. First we consider the following inequality

$$e^{2\alpha ky}-e^{-2\alpha ky}=\int_{-2\alpha ky}^{+2\alpha ky}e^{\zeta}\,d\zeta\le 4\,\alpha\,k\,y\,e^{2\alpha ky}, \tag{5.23}$$

and then we use it to find an upper bound for the sum of the series in (5.21). We write

$$\begin{aligned}0\le\frac{1}{y}\sum_{k=1}^{+\infty}k\,e^{-\alpha k^2}\left(e^{2\alpha ky}-e^{-2\alpha ky}\right)&\le 4\alpha\sum_{k=1}^{+\infty}k^2\,e^{-\alpha k^2}e^{2\alpha ky}\\ \le 4\alpha\sum_{k=1}^{+\infty}k^2\,e^{-\alpha k}e^{2\alpha ky}&=4\alpha\sum_{k=1}^{+\infty}k^2\,e^{-k\alpha(1-2y)},\end{aligned} \tag{5.24}$$

with $0<y<1/2$. We know from Lemma 5.1 that the last term goes to 0 for $\alpha\to+\infty$. This proves (5.21). Combination of (5.19), (5.20) and (5.21) proves (5.18) and hence claim (5.17). □

If we adopt again the old variables x and ϑ, see (5.10), the result of Theorem 5.2 can be rewritten as

$$S_x(\vartheta)\approx g(x,\vartheta),\qquad(\vartheta\downarrow 0), \tag{5.25}$$

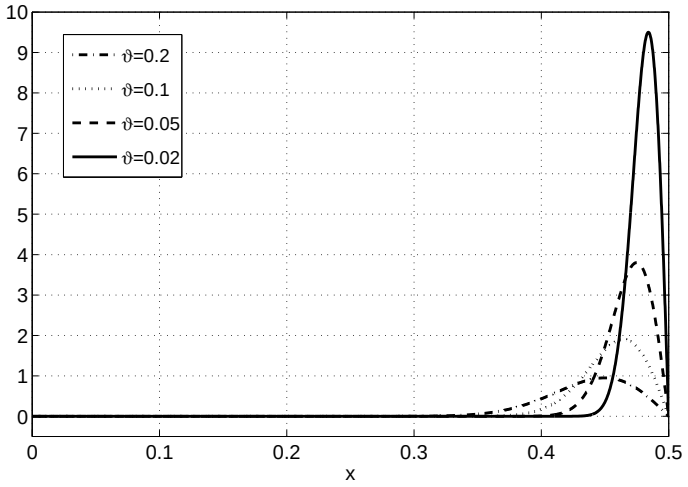

Figure 5: Plot of $g(x,\vartheta)$ as a function of x for different values of ϑ. The graph is drawn for $\gamma = 0.5$.

with

$$g(x,\vartheta) := \frac{\pi^{3/2}}{4\,\vartheta^{3/2}} \left(1 - \frac{x}{\gamma}\right) e^{-\pi^2(1-x/\gamma)^2/\vartheta} \tag{5.26}$$

and $0 < x < \gamma$. In Figure 5, $g(x,\vartheta)$ is plotted as a function of x for different values of ϑ. Equivalence (5.25) is used in the proof of the following theorem.

Theorem 5.3
$S_x(\vartheta)$ *has the following properties:*

1) $S_x(\vartheta)$ *goes exponentially to zero as* $\vartheta \downarrow 0$*;*

2) $S_x(\vartheta)$ *goes exponentially to zero as* $\vartheta \downarrow 0$ *non uniformly on the interval* $0 < x < \gamma$*;*

3) *given a constant* ϵ *independent of* x *and* ϑ *and such that* $0 < \epsilon < \gamma$, $S_x(\vartheta)$ *goes exponentially to zero as* $\vartheta \downarrow 0$ *uniformly on the interval* $0 < x < \gamma - \epsilon$.

Proof. Claim 1) can be proved using equivalence (5.25) and the fact that g goes exponentially to zero as $\vartheta \downarrow 0$.

For proving Claim 2), it is sufficient to show that

$$\sup_{0<x<\gamma} |S_x(\vartheta)|$$

is not limited for $\vartheta \downarrow 0$. For $0 < x < \gamma$ and any fixed $\vartheta > 0$, g is only a function of x, it is always positive and it has exactly one maximum (see Figure 5), i.e.

$$g_{max} := g(x_{max}) = \sqrt{\frac{\pi}{2\,e}}\,\frac{1}{4\,\vartheta}, \tag{5.27}$$

with

$$x_{max} := \gamma \left(1 - \frac{\sqrt{\vartheta}}{\sqrt{2}\,\pi}\right). \tag{5.28}$$

Clearly g_{max} is not limited for $\vartheta \downarrow 0$. As a consequence, because of equivalence (5.25), also the supremum of $S_x(\vartheta)$ is not limited for $\vartheta \downarrow 0$ and $0 < x < \gamma$. This proves Claim 2).

For proving Claim 3), we have to show that, for $0 < \epsilon < \gamma$ and in the limit for $\vartheta \downarrow 0$,

$$\sup_{0<x<\gamma-\epsilon} |S_x(\vartheta)|$$

remains limited. On the left of x_{max}, the function g is positive and monotonically increasing (see again Figure 5). Moreover we note that

$$\lim_{\vartheta \downarrow 0} x_{max} = \gamma. \tag{5.29}$$

Hence, for $0 < \epsilon < \gamma$, the following identity holds in the limit for $\vartheta \downarrow 0$

$$\sup_{0<x<\gamma-\epsilon} g(x,\vartheta) = g(\gamma-\epsilon,\vartheta). \tag{5.30}$$

The right hand side of (5.30) is limited for any positive value of ϑ and it goes to zero as $\vartheta \downarrow 0$. Because of that and of equivalence (5.25), we deduce Claim 3). □

At this point we have studied the properties of $S_x(\vartheta)$ for $\vartheta \downarrow 0$. The results found for $S_x(\vartheta)$ are used to state the properties of $\|M_{iter}\|_\infty$ for $\vartheta \downarrow 0$.

Theorem 5.4
Consider the LDC method for the one-dimensional heat problem (4.1)*. Consider the settings described in Section 4. In particular, let* Ω^H *be a uniform coarse grid with grid size* H *and, in* Ω^H*, approximate the second space derivative by the standard three-point finite differences scheme. Perform the temporal discretization with the backward Euler scheme and time step* Δt*. Let the local region be* $\Omega_l = (0,\gamma)$*, with* γ *a multiple of* H *such that* $0 < \gamma < 1$*. Locally replace the discretized operator* M_l^h *with the continuous operator* (4.4)*. Moreover, let* ϵ *be a constant independent of* x *and* ϑ*, and such that* $H < \epsilon < \gamma$*. Finally, let* Ω^H_{def}*, the subset of* Ω^H_l *in which an approximation of the local discretization error is computed, be given by*

$$\Omega^H_{def} = (0,\gamma-\epsilon) \cap \Omega^H_l. \tag{5.31}$$

Then, the following results hold for $\|M_{iter}\|_\infty$*:*

1) for any $H \geq 0$*,* $\|M_{iter}\|_\infty$ *goes exponentially to zero as* $\Delta t \downarrow 0$*;*

2) for any $H \geq 0$*,* $\|M_{iter}\|_\infty$ *goes exponentially to zero as* $\Delta t \downarrow 0$ *uniformly on* Ω^H_{def}*.*

Proof. For Δt small enough, combination of (5.1) with (4.37), (4.38) and (4.39) yields

$$\|M_{iter}\|_\infty \leq \|M_2\|_\infty \leq \frac{\pi\Delta t}{\gamma}\left|S_x\left(\frac{\pi^2\vartheta}{\gamma^2}\right)\right| + \frac{\pi}{6\gamma^2}\frac{H^2}{\Delta t}\left|S_\xi\left(\frac{\pi^2\Delta t}{\gamma^2}\right)\right|, \tag{5.32}$$

with $x \in \Omega^H_{def}$, $x - H < \xi < x + H$ and $0 < \vartheta < \Delta t$. Claims 1) and 2) follow immediately using the results of Theorem 5.3. □

The fact that the norm of the iteration matrix goes to zero as $\Delta t \downarrow 0$ is very natural. We expect this to happen in general and not only for the model problem considered here. We explain this as follows: if the time step Δt becomes extremely small, the solution at the new time step becomes very close to the solution at the previous time level. In such a situation, there is little to be corrected in the approximation at the new time step and, as a consequence, the LDC convergence rate is extremely fast.

As a final remark, we note that one basic assumption in the proof of Theorem 5.4 is the use of a safety region. As discussed later in Sections 5.3 and 6, this assumption is essential to have an exponential rate of convergence for $\Delta t \to 0$. Nevertheless, the LDC method turns out to be convergent also if the extent of the safety region is zero. This is similar to what happens in stationary cases. In [1, 3] the LDC iteration error for a 2D Poisson problem is proved to reduce proportionally to H^2 if $\epsilon > 0$. However, LDC is shown to be convergent (at a lower rate) also if $\epsilon = 0$.

5.2 The stationary case limit

In the limit case $\Delta t \to +\infty$, we expect the LDC convergence rate for the 1D heat equation to be the same as the LDC convergence rate for the one-dimensional Poisson equation. When LDC is applied to a 1D Poisson problem in combination with centered differences or any other method that integrates linear functions exactly, the method reaches a fixed point in one iteration for any grid size $H > 0$. (If $H = 0$, the stationary problem is solved exactly and there is no need to use LDC). This is proved in [4] and means that, in such a case, the iteration matrix is zero.

In the following theorem we provide a bound for $\|M_{\text{iter}}\|_\infty$ that holds in the limit for $\Delta t \to +\infty$ and any grid size $H > 0$. Clearly our results for the one-dimensional heat equation fit into the theory of LDC for 1D stationary problems.

Theorem 5.5
Consider the LDC method for the one-dimensional heat problem (4.1)*. Consider the settings described in Section 4 and a grid size* $H > 0$*. Then, for any* γ *such that* $0 < \gamma < 1$*, there exists a constant* C *such that*

$$\|M_{iter}\|_\infty \leq \frac{C}{\Delta t^2}, \quad (\Delta t \to +\infty). \tag{5.33}$$

Proof. For $\Delta t > 1$, combination of definition (3.13) with the result of Theorem 4.3 yields

$$\|M_{\text{iter}}\|_\infty \leq \frac{1}{\Delta t} \|M_2\|_\infty. \tag{5.34}$$

Hence, for proving Theorem 5.5 it is sufficient to show that, for any $\gamma \in (0,1)$, there exists a constant C such that

$$\|M_2\|_\infty \leq \frac{C}{\Delta t}, \quad (\Delta t \to +\infty). \tag{5.35}$$

We consider M_2 as expressed by (4.36) and we write

$$\|M_2(x)\|_\infty \leq \|S_1\|_\infty + \|S_2\|_\infty + \left\|S_{\text{poly}}\right\|_\infty, \tag{5.36}$$

with

$$S_1 := \frac{1}{\Delta t} \sum_{m=1}^{\infty} \nu_m e^{-m^2\pi^2\Delta t/\gamma^2} \sin\left(\frac{m\pi x}{\gamma}\right), \tag{5.37}$$

$$S_2 := \frac{4}{H^2} \sum_{m=1}^{\infty} \nu_m e^{-m^2\pi^2\Delta t/\gamma^2} \sin\left(\frac{m\pi H}{2\gamma}\right) \sin\left(\frac{m\pi x}{\gamma}\right), \tag{5.38}$$

$$S_{\text{poly}} := \frac{1}{\Delta t}\left(\frac{1}{6\gamma}x^3 - \frac{\gamma}{6}x\right). \tag{5.39}$$

With ν_m given by (4.32), we prove that $\|S_1\|_\infty$ and $\|S_2\|_\infty$ are $o(1/\Delta t)$, $(\Delta t \to +\infty)$. We start from S_2. We write

$$\begin{aligned} \|S_2\|_\infty &\leq \frac{4}{H^2} \sum_{m=1}^{\infty} |\nu_m| \left|e^{-m^2\pi^2\Delta t/\gamma^2}\right| \left|\sin\left(\frac{m\pi H}{2\gamma}\right)\right| \left\|\sin\left(\frac{m\pi x}{\gamma}\right)\right\|_\infty \\ &\leq \frac{8\gamma^2}{\pi^3 H^2} \sum_{m=1}^{\infty} \left|e^{-m\pi^2\Delta t/\gamma^2}\right| = \frac{8\gamma^2}{\pi^3 H^2} \frac{e^{-\pi^2\Delta t/\gamma^2}}{1 - e^{-\pi^2\Delta t/\gamma^2}}. \end{aligned} \tag{5.40}$$

For any $H > 0$ and any $\gamma \in (0,1)$, the last term in (5.40) is $o(1/\Delta t)$, $(\Delta t \to +\infty)$. A similar procedure can be used to show that $\|S_1\|_\infty$ is $o(1/\Delta t)$, $(\Delta t \to +\infty)$. Having

proved that two of the terms on the right hand side of (5.36) are $o(1/\Delta t)$, $(\Delta t \to +\infty)$, we deal now with the third one. Clearly, with the assumptions made, $\left\|S_{poly}\right\|_\infty$ is $\mathcal{O}(1/\Delta t)$, $(\Delta t \to +\infty)$. Therefore, there exists a constant C such that

$$\left\|S_{poly}\right\|_\infty \leq \frac{C}{\Delta t}, \quad (\Delta t \to +\infty). \tag{5.41}$$

This completes our proof. □

5.3 Plots of the iteration matrix norm

In Sections 5.1 and 5.2 we studied the asymptotic behavior of $\|M_{iter}\|_\infty$ for $\Delta t \downarrow 0$ and $\Delta t \to +\infty$ and we found that, in both cases, the limit of $\|M_{iter}\|_\infty$ is zero. In other words, we know two limit situations in which the rate of convergence of LDC becomes extremely fast. This does not mean, however, that the LDC method always converges. In this section we provide arguments in favor of the conjecture that, for our model problem and settings, M_{iter} is less than one for any choice of H and Δt, and thus the LDC method is unconditionally convergent.

For the one-dimensional heat equation and the LDC settings discussed in Section 4, we can compute $M_{iter} \in \mathbb{R}$ explicitly. For that we use the original definition (3.13) and we express M_1 by (3.14), with M^H as in (4.3), and M_2 by (4.36). In Figure 6 we plot M_{iter} as a function of Δt for different values of H and for $\gamma = 0.5$. In Figure 6-(a) M_{iter} is computed with a safety region $\epsilon = 0.15$, while in Figure 6-(b) no safety region is adopted. We immediately note that in both cases the maximum of M_{iter} is always less than 1, which means that the LDC method is always convergent. Moreover, for small and big values of Δt, we observe that the asymptotic behavior is in agreement with the bounds stated in Theorems 5.4 and 5.5. For $\Delta t \gg 1$ indeed LDC iteration errors reduce proportionally to Δt^{-2}. When Δt tends to zero, M_{iter} goes very rapidly to zero if we use a safety zone, see Figure 6-(a). Figure 6-(b) indicates that we should expect LDC to be convergent also when no safety region is employed; in this case the iteration error reduces proportionally to Δt^2 when $\Delta t \downarrow 0$.

Figure 7 illustrates the dependency of M_{iter} with respect to H when $\epsilon = 0$ and $\Delta t \ll 1$. For fixed time step, M_{iter} is proportional to H^{-4}.

6 Numerical experiments

In this section we further verify the results of Theorems 5.4 and 5.5 by means of some numerical experiments. One of the assumptions in the analysis carried out in Sections 4 and 5 is that both the local grid size h and the local time step δt are zero. This assumption is introduced for analysis purposes only, namely for being able to find the analytical solution of the local problem (4.27). The numerical experiments in this section, performed with positive values of h and δt, will show that the results of Theorems 5.4 and 5.5 still hold for a discrete local problem. In this section we also test the influence of the safety region ϵ on the rate of convergence of the LDC method and we try to observe the convergence behavior of Figures 6 and 7 for a concrete example.

We consider the application of the LDC method to the one-dimensional heat problem

$$\begin{cases} \dfrac{\partial u(x,t)}{\partial t} = \lambda \dfrac{\partial^2 u(x,t)}{\partial x^2} + f(x,t), & \text{in } \Omega = (0,1), \text{ for } t > 0, \\ u(0,t) = u(1,t) = 0, & \text{for } t > 0, \\ u(x,0) = \exp\left(-50\,(x-0.25)^2\right), & \text{in } [0,1], \end{cases} \tag{6.1}$$

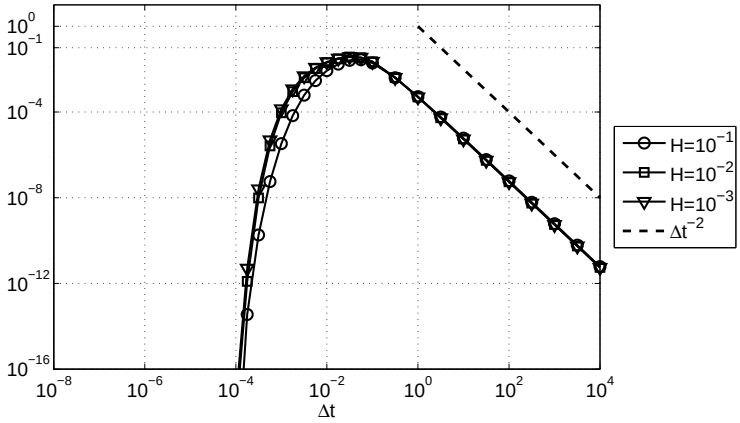

(a) Safety region $\epsilon = 0.15$

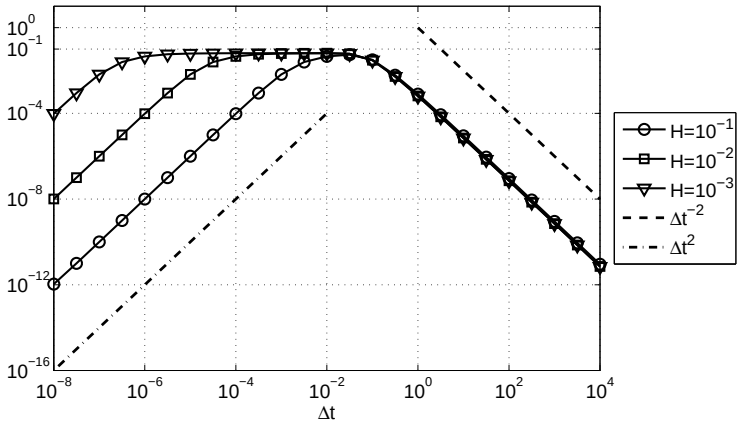

(b) No safety region ($\epsilon = 0$)

Figure 6: With reference to the model problem and settings of Section 4, plot of M_{iter} versus Δt for different values of H and for $\gamma = 0.5$; M_{iter} is computed explicitly from its definition.

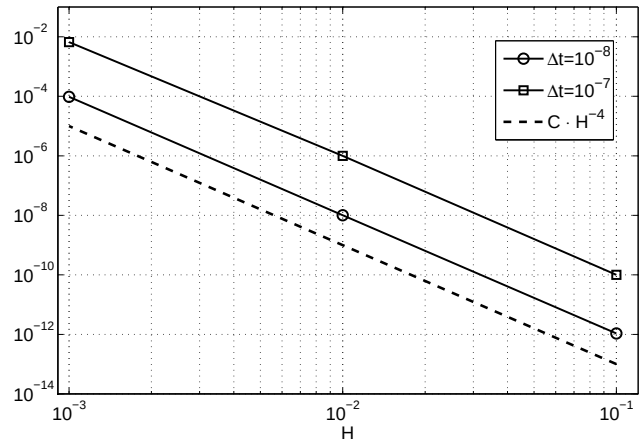

Figure 7: Plot of $M_{\text{iter}}(\Delta t = 10^{-8})$ and $M_{\text{iter}}(\Delta t = 10^{-7})$ as in Figure 6-(b) in terms of the grid size H.

with $\lambda = 0.01$ and

$$f(x,t) = 5\,\exp\left(-50\,\left(x - 0.05 + 0.15\,e^{-t}\right)^2\right). \tag{6.2}$$

In (6.1) the choice of initial condition, boundary conditions, diffusion coefficient and source term is such that the solution u has a region of high activity on the left half of the spatial domain. For this reason, we take the area of refinement as $\Omega_l = (0,\gamma)$, with $\gamma = 0.5$. In this way, as already noted before, the set Γ_H reduces to one point ($x = \gamma$) and M_{iter} to a real number. For the solution on the global coarse grid we adopt the same settings as in Section 4: the spatial discretization is performed by second-order centered differences, while the Euler backward scheme is used for the temporal discretization. For the solution on the local fine grid we employ the same numerical schemes as on the global coarse grid.

We run tests aimed at measuring the convergence rate of the LDC method during one time step. We adopt the following strategy: starting from the initial condition, we perform one LDC time step with a chosen grid size H and a chosen time step Δt. The local grid size and time step are taken as $h = H/5$ and $\delta t = \Delta t/5$. For measuring M_{iter}, we act as follows: at every LDC iteration, we store the coarse grid solution on the interface Γ^H. We say that the LDC iteration has converged when

$$|u^{H,1}_{\Gamma,w} - u^{H,1}_{\Gamma,w-1}| < \text{tolerance}, \tag{6.3}$$

for a certain $w \geq 1$. In (6.3), $u^{H,1}_{\Gamma,w}$ denotes the solution on Γ^H after one time step and w LDC iterations. In our numerical experiments, we set the value of the tolerance to 10^{-12}. Once the converged value on the interface is known, the error $e^H_{\Gamma,w}$ can be computed for every iteration w that has been performed. Finally, see (3.11), M_{iter} is given by

$$M_{\text{iter}} = \frac{e^H_{\Gamma,w}}{e^H_{\Gamma,w-1}}, \tag{6.4}$$

for a certain $w \geq 1$. In practice we take $w = 1$ in (6.4). Note that, if the LDC method converges in exactly one iteration, $M_{\text{iter}} = 0$.

We run two series of experiments on problem (6.1), the first one with a safety region, the second one with no safety region. The results are displayed in Figure 8. In Figure 8-(a) M_{iter} is plotted as a function of Δt for different values of the coarse grid size H. Except for the fact that the local problem is not solved analytically but numerically, in this numerical experiment all the assumptions of Theorems 5.4 and 5.5 are satisfied. Note that the extent of the safety region ($\epsilon = 0.1$) is greater than H, for every H considered. As expected, M_{iter} goes very rapidly to zero for small values of Δt while, for big values of the time step, iteration errors reduce proportionally to Δt^{-2}. For each value of H considered in the experiment, the maximum of M_{iter} is always below 10^{-1}; this means that, even in the worst case, the error $e^H_{\Gamma,w}$ is reduced by a factor bigger than 10 at every LDC iteration. Figure 8-(b) refers to the experiment with no safety region. The behavior for $\Delta t \gg 1$ is the same as before; in Theorem 5.5, in fact, no assumption is made on the extent of ϵ. For $\Delta t \ll 1$ iteration errors reduce proportionally to Δt^2. Note that, also in this case, the maximum of M_{iter} is always below 10^{-1}. Overall the graphs in Figure 8 are qualitatively very similar to the ones in Figure 6, where M_{iter} was computed directly from the definition (3.13). In Figure 9 we finally plot, as a function of H, the values of M_{iter} as they are computed by solving problem (6.1) with $\Delta t = 10^{-4}$ and $\epsilon = 0$. As already illustrated in Figure 7, with fixed (and small) Δt and no safety region, M_{iter} is $\mathcal{O}(H^{-4})$.

So far we have only considered pure diffusion problems. Here we would also like to investigate, by means of a numerical experiment, the LDC rate of convergence when

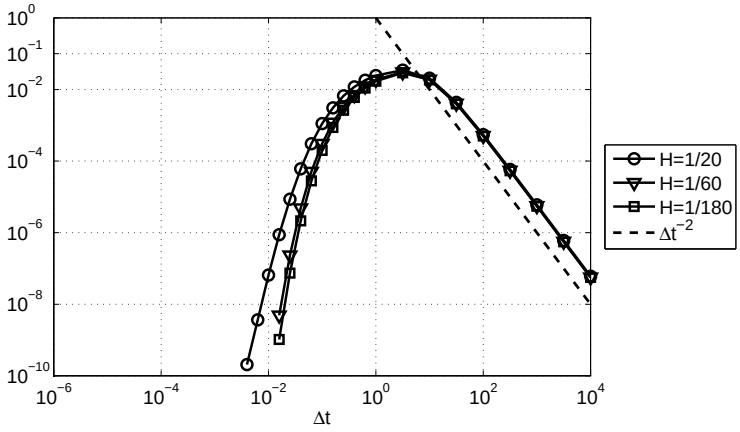

(a) Safety region $\epsilon = 0.1$

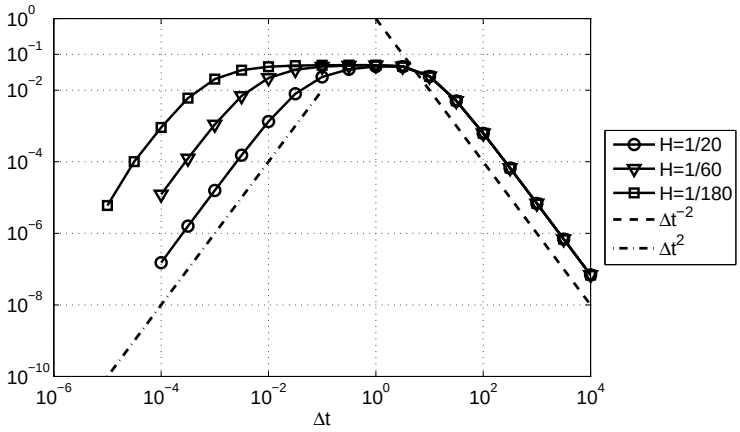

(b) No safety region ($\epsilon = 0$)

Figure 8: Plot of $M_{\text{iter}}(\Delta t)$ for different values of H as computed by solving the heat problem (6.1).

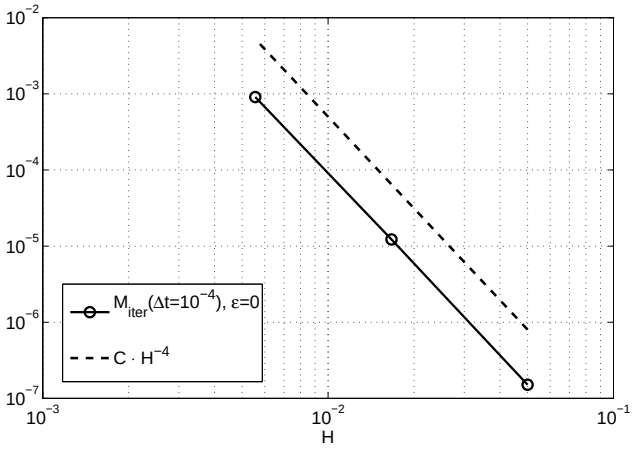

Figure 9: Plot of $M_{\text{iter}}(\Delta t = 10^{-4})$ as in Figure 8-(b) in terms of the grid size H.

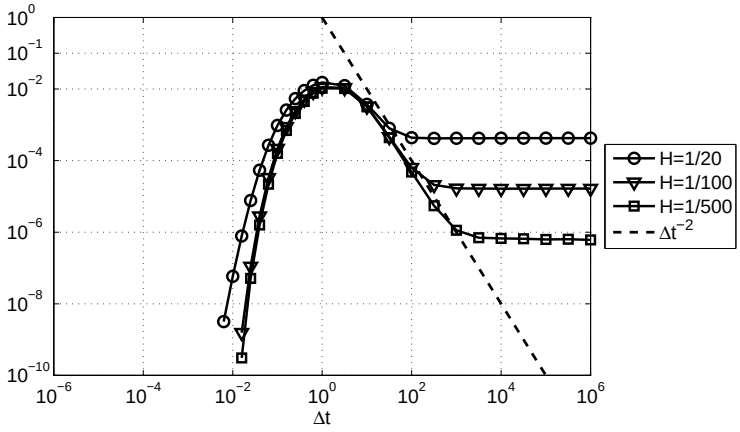

(a) Safety region $\epsilon = 0.1$

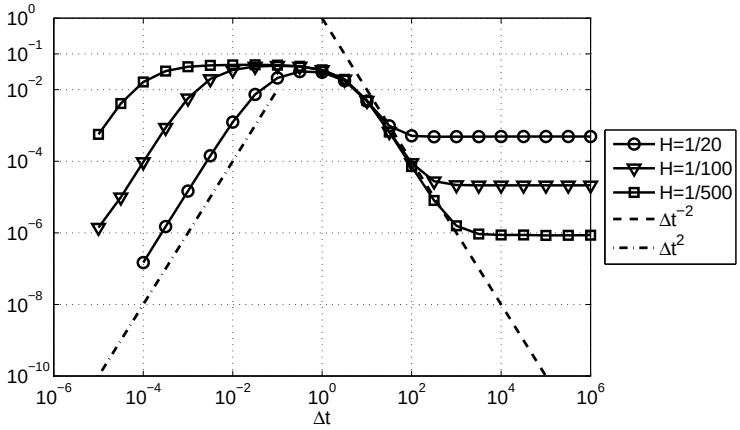

(b) No safety region ($\epsilon = 0$)

Figure 10: Plot of $M_{iter}(\Delta t)$ for different values of H as computed by solving the convection-diffusion equation (6.5).

the method is applied to a one-dimensional convection-diffusion problem. We consider the following partial differential equation

$$\frac{\partial u(x,t)}{\partial t} + \nu \frac{\partial u(x,t)}{\partial x} = \lambda \frac{\partial^2 u(x,t)}{\partial x^2} + f(x,t), \quad \text{in } \Omega = (0,1), \text{ for } t > 0, \tag{6.5}$$

with $\nu = -0.1$. Equation (6.5) is solved with the same initial condition, boundary conditions, diffusion coefficient and source term as problem (6.1). Moreover the same numerical schemes and local region are adopted as before, and the same strategy to compute M_{iter} is employed. Note that in (6.5) convection is the main way of heat transport since the relative weight of convection with respect to diffusion is

$$\frac{|\nu|}{\lambda} = \frac{0.1}{0.01} = 10. \tag{6.6}$$

Like before, we run two sets of numerical experiments, one with a safety region $\epsilon = 0.1$ and another one with no safety region. The results are displayed in Figure 10. For small values of the time step Δt the rate of convergence M_{iter} has the same behavior as for pure diffusion problems. Also the maximum value of $M_{iter}(\Delta t)$ is, for

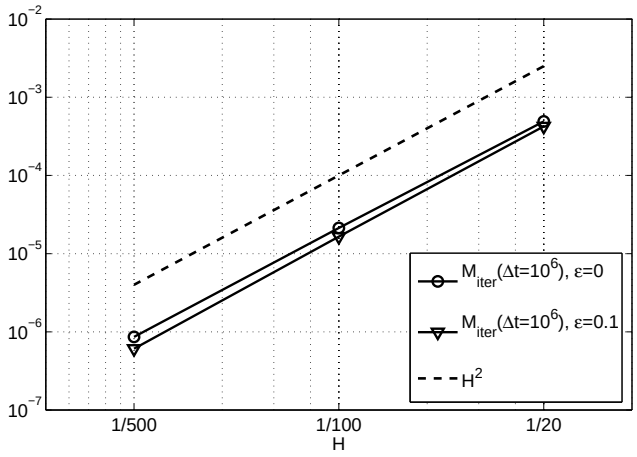

Figure 11: Plot of $M_{\text{iter}}(\Delta t = 10^6)$ as in Figure 10 in terms of the grid size H.

every H, about the same (less than 10^{-1}) as observed before. For big values of Δt, however, we note that M_{iter} first decreases as $\mathcal{O}(\Delta t^{-2})$, but then an asymptotic value (greater than 0) is reached. To illustrate the dependency of the asymptotic value on the grid size, in Figure 11 we plot, as a function of H, $M_{\text{iter}}(\Delta t = 10^6)$ as computed in the two sets of experiments on problem (6.5). From the graph we can see that, in both cases, the asymptotic value is proportional to the square of the coarse grid size.

7 Conclusions

In this paper we studied the convergence properties of the Local Defect Correction method for parabolic problems. For a general two-dimensional case, we found an expression for the LDC iteration matrix: at a generic time step, the LDC iteration can be expressed in terms of an iteration that takes place on Γ^H only, with Γ^H the set of coarse grid points that lie on the interface between coarse and fine grid. If the iteration on Γ^H converges, then the entire LDC iteration reaches a fixed point.

For a one-dimensional heat equation and a particular choice for the grids and the discretization schemes, the properties of the iteration matrix can be studied in detail. The norm of the iteration matrix is proved to go exponentially to zero when the time step Δt goes to zero if we use a safety region. If no safety region is used, the norm of the iteration matrix reduces proportionally to Δt^2 for $\Delta t \downarrow 0$. The results of our analysis for time-dependent problems fit into the theory of LDC for stationary cases: in fact the norm of the iteration matrix goes to zero when $\Delta t \to +\infty$. The asymptotic analysis says that this happens proportionally to Δt^{-2}. Since the maximum of the iteration matrix norm turns out to be less than one for any choice of the grid size H, we claim that LDC applied to the solution of a one-dimensional heat equation is unconditionally convergent.

All the results of the theoretical analysis are verified by means of numerical experiments. Moreover, LDC applied to a one-dimensional convection-diffusion equation shows the same convergence behavior as for a pure diffusion problem. Only in the stationary case limit we observe differences: in the problem with a convection term the iteration matrix norm does not go to zero, but it reaches an asymptotic value proportional to the square of the coarse grid size.

References

[1] M. J. H. Anthonissen. *Local defect correction techniques: analysis and application to combustion*. PhD thesis, Eindhoven University of Technology, Eindhoven, 2001.

[2] M. J. H. Anthonissen. Local defect correction techniques applied to a combustion problem. In R. Kornhuber, R. Hoppe, J. Périaux, O. Pironneau, O. Widlund, and J. Xu, editors, *Domain Decomposition Methods in Science and Engineering*, Lecture Notes in Computational Science and Engineering, pages 185–192, Berlin, Heidelberg, New York, 2005. Springer.

[3] M. J. H. Anthonissen, R. M. M. Mattheij, and J. H. M. ten Thije Boonkkamp. Convergence analysis of the local defect correction method for diffusion equations. *Numerische Mathematik*, 95:401–425, 2003.

[4] M. J. H. Anthonissen and R. Minero. Conditions for one-step convergence of the local defect correction method for elliptic problems. Technical Report CASA 05-39, Eindhoven University of Technology, Eindhoven, November 2005.

[5] M. J. H. Anthonissen, B. van 't Hof, and A. A. Reusken. A finite volume scheme for solving elliptic boundary value problems on composite grids. *Computing*, 61:285–305, 1998.

[6] L. K. Bieniasz. Use of dynamically adaptive grid techniques for the solution of electrochemical kinetic equations: Part 5. A finite-difference, adaptive space/time grid strategy based on a patch-type local uniform spatial grid refinement, for kinetic models in one-dimensional space geometry. *Journal of Electroanalytical Chemistry*, 481:115–133, 2000.

[7] P. J. J. Ferket. Coupling of a global coarse discretization and local fine discretizations. In W. Hackbusch and G. Wittum, editors, *Numerical Treatment of Coupled Systems*, volume 51 of *Notes on Numerical Fluid Mechanics*, pages 47–58, Braunschweig, 1995. Vieweg.

[8] P. J. J. Ferket. *Solving boundary value problems on composite grids with an application to combustion*. PhD thesis, Eindhoven University of Technology, Eindhoven, 1996.

[9] P. J. J. Ferket and A. A. Reusken. Further analysis of the local defect correction method. *Computing*, 56:117–139, 1996.

[10] P. J. J. Ferket and A. A. Reusken. A finite difference discretization method on composite grids. *Computing*, 56:343–369, 1996.

[11] M. Graziadei, R. M. M. Mattheij, and J. H. M. ten Thije Boonkkamp. Local defect correction with slanting grids. *Numerical Methods for Partial Differential Equations*, 20:1–17, 2003.

[12] W. Hackbusch. Local defect correction and domain decomposition techniques. In K. Böhmer and H. J. Stetter, editors, *Defect Correction Methods. Theory and Applications, Computing, Suppl. 5*, pages 89–113, Wien, New York, 1984. Springer.

[13] R. Minero, M. J. H. Anthonissen, and R. M. M. Mattheij. Local defect correction for time-dependent partial differential equations. In *Proceedings of the 16th International Conference on Domain Decomposition Methods*, 2005. Available online at http://cims.nyu.edu/dd16/proceedings.html.

[14] R. Minero, M. J. H. Anthonissen, and R. M. M. Mattheij. A local defect correction technique for time-dependent problems. *Numerical Methods for Partial Differential Equations*, 2006. Early view.

[15] R. Minero, M. J. H. Anthonissen, and R. M. M. Mattheij. Solving parabolic problems using local defect correction in combination with the finite volume method. *Numerical Methods for Partial Differential Equations*, 2006. In press.

[16] V. Nefedov and R. M. M. Mattheij. Local defect correction with different grid types. *Numerical Methods for Partial Differential Equations*, 18:454–468, 2002.

[17] D. Norman. *Introduction to Linear Algebra for Science and Engineering*. Addison-Wesley Publishers Limited, 1995.

[18] I. E. M. Severens, M. J. H. Anthonissen, R. M. M. Mattheij, and J. M. L. Maubach. Application of the local defect correction method in discrete element method simulations. Technical Report CASA 04-17, Eindhoven University of Technology, Eindhoven, August 2004.

[19] C. R. Traas, H. G. ter Morsche, and R. M. J. van Damme. *Splines en Wavelets*. Epsilon Uitgaven, Utrecht, 2000. In Dutch.

[20] R. A. Trompert. Local uniform grid refinement and systems of coupled partial differential equations. *Applied Numerical Mathematics*, 13:251–270, 1993.

[21] R. A. Trompert and J. G. Verwer. Analysis of the implicit Euler local uniform grid refinement method. *SIAM Journal on Scientific Computing*, 14:259–278, 1993.

[22] R. A. Trompert and J. G. Verwer. Runge-Kutta methods and local uniform grid refinement. *Mathematics of Computation*, 60:591–616, 1993.

[23] J. U. Wappler. *Die lokale Defektkorrekturmethode zur adaptiven Diskretisierung elliptischer Differentialgleichungen mit finiten Elementen*. PhD thesis, Christian-Albrechts-Universität, Kiel, 1999. In German.